BIOCHEMISTRY
including biophysical chemistry & molecular biology

ARTICLE

pubs.acs.org/biochemistry

Effect of Hydrogen Bond Strength on the Redox Properties of Phylloquinones: A Two-Dimensional Hyperfine Sublevel Correlation Spectroscopy Study of Photosystem I

Nithya Srinivasan,[†] Ruchira Chatterjee,[§] Sergey Milikisiyants,[§] John H. Golbeck,[†,‡] and K. V. Lakshmi*[,§]

[†]Department of Biochemistry and Molecular Biology, The Pennsylvania State University, University Park, Pennsylvania 16802, United States

[‡]Department of Chemistry, The Pennsylvania State University, University Park, Pennsylvania 16802, United States

[§]Department of Chemistry and Chemical Biology and The Baruch '60 Center for Biochemical Solar Energy Research, Rensselaer Polytechnic Institute, Troy, New York 12180, United States

Supporting Information

ABSTRACT: The phylloquinones of photosystem I (PS I), A_{1A} and A_{1B}, exist in near-equivalent protein environments but possess distinct thermodynamic and kinetic properties. Although the determinants responsible for the different properties of the phylloquinones are not completely understood, the strength and geometry of hydrogen bond interactions are significant factors in tuning and control of function. This study focuses on characterizing the hydrogen-bonding interactions of the phylloquinone acceptor, A_{1A}, by ^{1}H and ^{14}N HYSCORE spectroscopy. Photoaccumulation of PS I complexes at pH 8.0 results in the trapping of the phyllosemiquinone anion, A_{1A}^{-}, on the A-branch of cofactors. The experiments described here indicate that A_{1A}^{-} forms a single H-bond. Using a simple point dipole approximation, we estimate its length to be 1.6 ± 0.1 Å. The value of the ^{1}H isotropic hyperfine coupling constant suggests that the H-bond has significant out-of-plane character. The ^{14}N HYSCORE spectroscopy experiments support the assignment of a H-bond wherein, the ^{14}N quadrupolar coupling constant is consistent with a backbone amide nitrogen as the hydrogen bond donor.

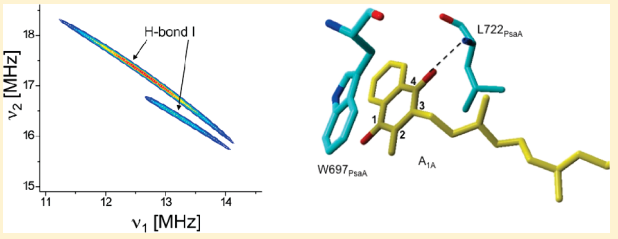

The primary purpose behind efforts to obtain more refined spectroscopic and high-resolution structural data of cofactor binding sites within photosynthetic reaction center complexes is to better understand how structural and magnetic properties relate to biological function. The phylloquinones in the A_{1A} and A_{1B} sites of photosystem I (PS I) are difficult to distinguish because they exist in near-equivalent protein environments. Nevertheless, advances in time-resolved optical spectroscopy and electron paramagnetic resonance (EPR) spectroscopy, combined with site-directed mutagenesis, have enabled the distinction between the A_{1A} and A_{1B} phylloquinones. The electron transfer properties of the two phylloquinones are distinct; the A_{1A}^{-} phyllosemiquinone transfers the electron to F_X in ~200 ns while A_{1B}^{-} transfers the electron to F_X in ~20 ns.[1] While the electron transfer from A_{1A}^{-} is strongly activated and slows down as the temperature is lowered, electron transfer from A_{1B}^{-} is temperature independent.[2,3] The current model that explains these observations posits that electron transfer on the A-branch of PS I is thermodynamically uphill while electron transfer on the B-branch is thermodynamically downhill, implying that A_{1A} is more oxidizing than A_{1B}. This model is supported by computational studies, which indicate that A_{1B} is 155–173 mV more reducing than A_{1A}.[4,5] These observations beg the obvious question as to why two chemically identical molecules possess such diverse electron transfer properties. Although it is expected that the protein environment plays a major role in modulating the redox properties of the quinones, the determinants that cause this large difference between the A_{1A} and A_{1B} phylloquinone acceptors of PS I are incompletely understood.

Based on the 2.5 Å resolution X-ray crystal structure of PS I (PDB ID: 1JB0),[6] two important interactions between the A- and B-branch phylloquinones and the protein environment can be identified, namely, a π-stacking interaction with a Trp residue and hydrogen (H) bonding with a Leu residue (Figure 1). The single H-bond formed between the C_4 carbonyl keto oxygen atoms of the phylloquinone molecule and the backbone amide peptide group of a Leu residue plays a key role in maintaining the functional integrity of the binding pocket.[7] However, the X-ray crystal structure of PS I[6] details the molecular interactions of the A_{1A} and A_{1B} acceptors only in the neutral state. These interactions could be significantly different in the reduced semiquinone states, A_{1A}^{-} and A_{1B}^{-}. Hence, it is important to conduct electron

Received: December 24, 2010
Revised: March 9, 2011
Published: April 08, 2011

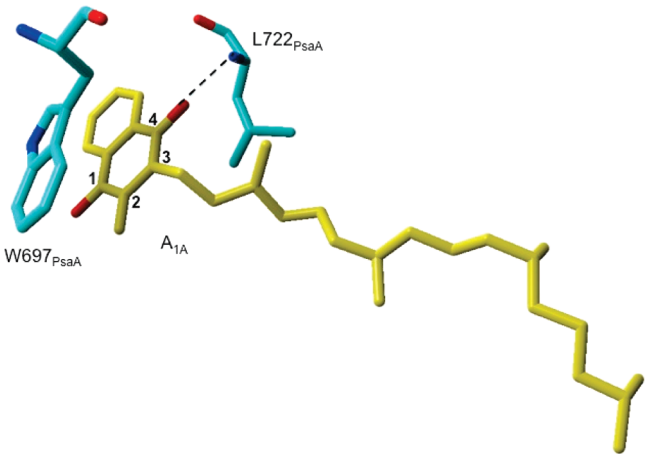

Figure 1. A-branch phylloquinone binding pocket showing the H-bonded $L722_{PsaA}$ and the π-stacked $W697_{PsaA}$ residues. The quinone headgroup has been numbered to facilitate identification of the ring carbons.

paramagnetic resonance (EPR) spectroscopy studies to directly probe the strength and geometry of the H-bonds in their state.

The electron−nuclear hyperfine interactions of the reduced phyllosemiquinone with the proton nuclei of the surrounding protein matrix have previously been probed by electron nuclear double resonance (ENDOR) spectroscopy. The chemical reduction of PS I with sodium hydrosulfite at pH 8.0, followed by brief illumination at 205 K, was shown to fully reduce F_A/F_B, partly reduce F_X, and somewhat reduce A_1.[8] Longer periods of illumination resulted in the complete reduction of F_X, ultimately generating one spin from "A_1^-" per P_{700} in PS I.[8] Under these conditions, ENDOR studies have revealed the presence of a proton hyperfine interaction of the phyllosemiquinone with an isotropic hyperfine interaction, a_{iso}, of 10.3 and 10.2 MHz in PS I complexes from *Anabena variabilis* and spinach, respectively.[9] In each case, the observed isotropic hyperfine interaction has been assigned to the methyl ($-CH_3$) group at the C_2 position of the phyllosemiquinone state, A_1^-. These values of a_{iso} for the hyperfine interaction to the methyl ($-CH_3$) group of the phyllosemiquinone of PS I are significantly higher than the a_{iso} value of 7.9 MHz that has been observed for the phyllosemiquinone anion radical in vitro (in alkaline methanol).[9] The larger isotropic hyperfine coupling constants that are observed for the PS I-bound phyllosemiquinone have been attributed to the presence of an unusually high electron spin density at the C_2 position.

The ENDOR study[9] also reported additional hyperfine couplings arising from protons that were H-bonded to the semiquinone. The findings suggested that the quinone might form two H-bonds, one with each carbonyl keto oxygen atom. The values for a_{iso} that were reported for the two H-bonds in *A. variabilis* and spinach were 1.13, 0.60 and 1.00, 0.47, respectively. The ENDOR studies conducted on PS I isolated from *Chlamydomonas reinhardtii* under different photoaccumulation conditions had indentified a similar H-bonding pattern to both A_{1A}^- and A_{1B}^-.[10,11] However, these findings have been questioned on theoretical grounds.[12] The observed difference in the a_{iso} values and hence the relative strengths of the H-bond obtained from ENDOR spectroscopy do not sufficiently account for the high electron spin density at the C_2 position that results in larger isotropic hyperfine coupling constants that are observed for the methyl group. Furthermore, it should be noted that the detection of a second H-bond by ENDOR spectroscopy is not supported by transient EPR spectroscopy studies on selectively ^{13}C-labeled naphthoquinones, which suggest only a single H-bond to the A_{1A}^- semiquinone.[13,14] Additional evidence for the presence of a single H-bond to the semiquinone, A_{1A}^- has been obtained from pulsed EPR, ENDOR, and TRIPLE studies performed at Q-band (34 GHz), which is better suited to study semiquinone radicals.[15,16] By the incorporation of deuterated phylloquinones in a background of protonated PS I, the hyperfine coupling tensor associated with only a single H-bond could be identified.[15] The magnitude of the measured dipolar tensor corresponds to an unusually short H-bond, estimated to be 1.5 ± 0.1 Å using a point-dipole approximation. These studies suggest that the resonance attributed to a second H-bond to A_{1A}^- in the X-band ENDOR studies[9−11] may have been derived instead from a proton associated with A_0^-. Thus, there is the need for unambiguous assignment of the strength and geometry of the H-bond(s) of the phyllosemiquinone(s) of PS I.

In this study, we use hyperfine sublevel correlation (HYSCORE) spectroscopy, a two-dimensional (2D) pulsed EPR spectroscopy technique, to probe the H-bonds to the phyllosemiquinone anion(s) of PS I. HYSCORE spectroscopy is a 2D electron spin-echo envelope modulation (ESEEM) technique in which the electron−nuclear hyperfine and quadrupole interactions of an electron spin (e.g., phyllosemiquinone, electron spin $S = 1/2$) with nuclear spins (e.g., ^1H and ^{14}N nuclei, nuclear spin $I = 1/2$ and 1, respectively) of the surrounding protein matrix are detected in 2D frequency space. The observation of the electron−nuclear magnetic interaction in 2D frequency space renders HYSCORE spectroscopy a powerful tool for high-resolution structure determination of paramagnetic systems. 2D ^1H and ^{14}N HYSCORE spectroscopy greatly enhances spectral resolution since the addition of a second dimension enables the detection of the hyperfine interactions in a much larger frequency space. Furthermore, in the case of a semiquinone anion, the nuclear frequencies are correlated in the two dimensions of the 2D ^1H and ^{14}N HYSCORE experiments, which simplify the analysis and the assignment of the hyperfine interactions. This allows for the unambiguous interpretation of the experimental spectra. While ENDOR spectroscopy is best suited to determine hyperfine interactions with directly bonded nuclei such as methyl protons, it provides an inaccurate estimate of highly anisotropic hyperfine couplings to H-bonded nuclei. This is because the latter are often masked by the hyperfine couplings with strongly interacting directly bonded intrinsic nuclei. The weak interactions which are masked in one-dimensional ENDOR and ESEEM spectroscopy experiments can often be detected in a 2D HYSCORE experiment due to enhanced spectral resolution.

Here, we report the study of the phyllosemiquinone, A_{1A}^-, using ^1H and ^{14}N HYSCORE spectroscopy. We confirm that A_{1A}^- forms one nonplanar H-bond with an a_{iso} of −0.27 MHz, which corresponds to a bond length of 1.6 ± 0.1 Å as estimated from a simple point-dipole approximation. Furthermore, we establish the identity of the H-bond by demonstrating that the H-bonding partner is a backbone amide group and obtain hyperfine and quadrupolar coupling constants for the backbone amide nitrogen atom. Thus, we demonstrate that 2D ^1H and ^{14}N HYSCORE spectroscopy can be used to obtain high-resolution structural parameters for the H-bonds of the phyllosemiquinone state of PS I.

MATERIALS AND METHODS

Preparation of PS I Complexes. The growth of *Synechocystis* sp. PCC 6803 wild-type cells and isolation of PS I complexes were performed as described in ref 17.

Generation of the A_{1A}^- Phyllosemiquinone State of PS I. The sample was incubated with 50 mM sodium dithionite under anaerobic conditions for 30 min to reduce the [4Fe−4S] clusters of PS I followed by illumination at low light intensities at 205 K for 10 min to photoaccumulate the A_{1A}^- phyllosemiquinone.[8,11]

Generation of the P_{700}^+ State of PS I. The PS I sample was incubated with 5 mM potassium ferricyanide to chemically oxidize the primary donor and generate the P_{700}^+ cation.[18]

2D ^{1}H and ^{14}N HYSCORE Spectroscopy. For the 2D HYSCORE spectra reported here, the pulsed echo amplitude was measured using the pulse sequence $(\pi/2-\tau-\pi/2-t_1-\pi-t_2-\pi/2-\text{echo})$ with a τ delay of 136 ns and a 12 ns detector gate (that is, centered at the maximum of the echo signal); the delays are defined as the differences in the starting point of the pulses. The echo intensity was measured as a function of t_1 and t_2, where t_1 and t_2 were incremented in steps of 16 ns from their initial values of 32 and 40 ns, respectively. The static magnetic field value and the microwave frequency were 345.7 mT and 9.707 GHz, respectively. A $\pi/2$ pulse of 8 ns and an equal amplitude, 16 ns π pulse were used to record a 384 × 384 matrix. The 8 ns time difference between the initial values of t_1 and t_2 and $\pi/2$ and π pulses were set to obtain more symmetric spectra. The application of a 16-step phase cycling procedure was used to eliminate the unwanted echoes and anti-echoes. The echo decay was eliminated by a low-order polynomial baseline correction and tapered with a Hamming function. Prior to 2D Fourier transformation, the data was zero-filled to a 2048 × 2048 matrix, and the magnitude spectra were calculated using the Bruker X-EPR software (Bruker BioSpin Corp., Billerica, MA). The spectra are presented as contour plots that were prepared in Matlab R2008a. All HYSCORE experiments were performed at 30 K.

Analysis of the 2D ^{1}H HYSCORE Spectra. The anisotropic (T) and isotropic (a_{iso}) component of the hyperfine interaction of the semiquinone with a H-bonded proton are obtained by analyzing the data as previously described.[19,20] In general, the three principal components of an electron−nuclear hyperfine tensor can be presented as $(a_{iso}- T(1-\delta), a_{iso} - T(1+\delta)$, and $a_{iso} + 2T)$, where a_{iso}, T, and δ are the isotropic, dipolar, and rhombic components of the tensor, respectively. When these are plotted in squared-frequency coordinates, in the case of axial symmetry ($\delta = 0$) in powder samples, the proton ridges represent straight line segments.[20] The anisotropic and isotropic components can be determined from the slope and the intercept of the ridges.[20] If the slope, $Q_{\alpha(\beta)}$, and the intercept, $G_{\alpha(\beta)}$, are determined experimentally, the values of a_{iso} and T can be calculated from following equations:[19]

$$T = \pm\sqrt{\frac{1G}{9(1-Q_{\alpha(\beta)})}\left\{G_{\alpha(\beta)} + \frac{4\nu_I{}^2 Q_{\alpha(\beta)}}{1-Q_{\alpha(\beta)}}\right\}}$$

and

$$a_{iso} = \pm 2\nu_I\frac{1+Q_{\alpha(\beta)}}{1-Q_{\alpha(\beta)}} - \frac{T}{2}$$

In principle, linear analysis provides several possible pairs of proton hyperfine parameters. Since 2D HYSCORE is only sensitive to the relative sign of the hyperfine components, it yields two possible options for the absolute sign. In addition, the slope and the intercept remain unchanged if the value of the parallel and perpendicular components of a_{iso} are interchanged and therefore provides two possible values for a_{iso}. The correct pair of hyperfine parameters can be selected if there is a literature reference as in the case of the methyl protons.[21] For the hydrogen bond, the multiple options can be easily resolved since in this case the hyperfine interaction is predominantly dipolar in nature and must result in nearly an axial point-dipole tensor with a positive value of T. Additional support is obtained from the numerical simulations of the 2D ^{1}H HYSCORE spectrum using the "saffron" function of the EasySpin software package.[22]

Numerical Simulations of 2D ^{14}N HYSCORE Spectra. The "saffron" function of the EasySpin software package was used for the numerical simulation of the experimental ^{14}N and ^{1}H HYSCORE spectrum.[22]

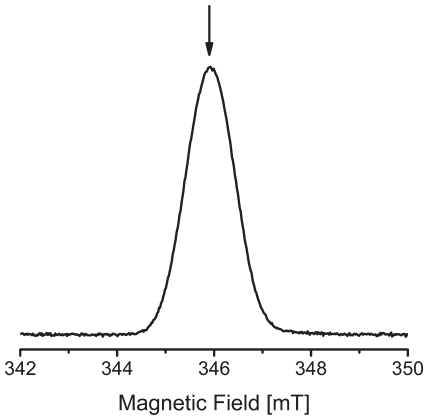

Figure 2. Electron spin-echo EPR spectrum of PS I trimers photoaccumulated at pH 8.0. The magnetic field position at which the 2D HYSCORE spectroscopy measurements were performed is indicated by an arrow.

RESULTS AND DISCUSSION

Figure 2 depicts the electron spin-echo EPR spectrum of PS I trimers (pH 8.0) photoaccumulated under low light intensity at 205 K. The EPR signal at $g \sim 2.0055$ with a spectral width of 1.4 mT is indicative of the presence of a phyllosemiquinone anion. It has previously been shown that under the photoaccumulation conditions employed here only the A_{1A}^- semiquinone state is generated.[8,11] The magnetic field value of 345.7 mT that corresponds to the maximum intensity of the EPR signal (as indicated by an arrow in Figure 2) was chosen to conduct subsequent 2D HYSCORE spectroscopy on the phyllosemiquinone.

Shown in Figure 3 is the (+,+) quadrant of the 2D ^{1}H HYSCORE spectrum of the phyllosemiquinone anion, A_{1A}^-, photoaccumulated at pH 8.0. The diagonal of the quadrant and the antidiagonal that intersects the diagonal at the ^{1}H Zeeman frequency of 14.7 MHz are also shown in Figure 3. The spectrum displays two symmetric pairs of extended cross-peaks (or ridges) located in the vicinity of the ^{1}H Zeeman frequency. The pairs of ridges in the 2D ^{1}H HYSCORE spectrum arise from the electron−nuclear hyperfine interactions of A_{1A}^- (electron spin $S = 1/2$) with neighboring ^{1}H nuclei (nuclear spin $I = 1/2$) in the binding pocket. The pair of ridges that is closest to the antidiagonal is attributed to hyperfine interactions arising from the

dx.doi.org/10.1021/bi102056q |*Biochemistry* 2011, 50, 3495–3501

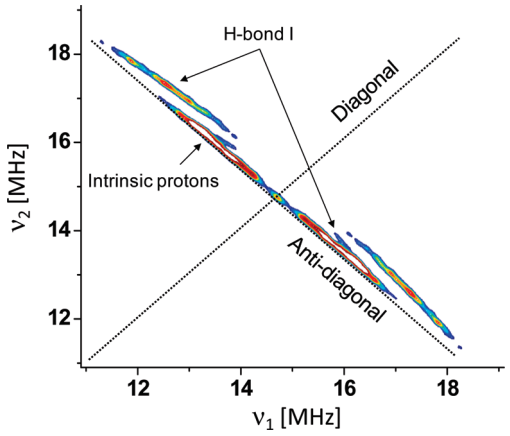

Figure 3. The (+,+) quadrant of the experimental 2D ^{1}H HYSCORE spectrum of PS I photoaccumulated at pH 8. Also shown are the diagonal and the antidiagonal of the quadrant, which intersects with the diagonal at the ^{1}H Zeeman frequency of 14.7 MHz.

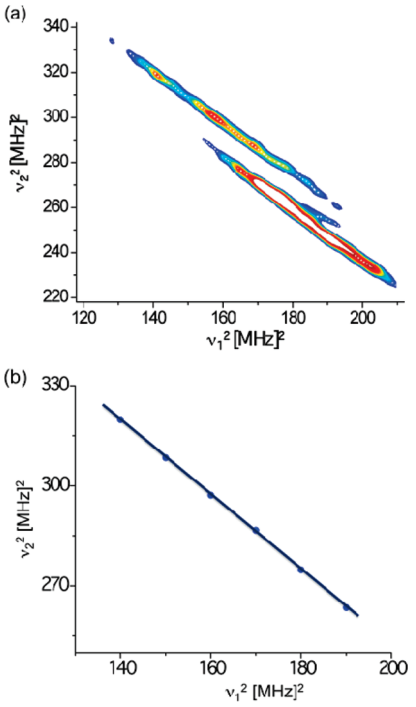

Figure 4. (a) Cross-peaks arising from the proton hyperfine interactions in PS I photoaccumulated at pH 8 plotted in the squared-frequency coordinate system. (b) A plot of selected points from line shape obtained in (a). The straight line indicates a linear fit to the experimental data points for H-bond I.

protons that are intrinsic to the phylloquinone, such as the ring protons and β-methylene protons of the phytyl tail. The spectrum also displays an additional pair of ridges that is shifted farther from the diagonal (Figure 1S, Supporting Information). This pair of ridges is attributed to the electron−nuclear hyperfine interaction of the three protons on the methyl group of the phyllosemiquinone anion. Analysis (not shown) of the cross-peaks provide an a_{iso} value of 9.94 ± 0.2 MHz and a T value of 1.33 ± 0.2 MHz for the methyl protons. These assignments are in excellent agreement with previously published literature.[16]

More importantly, the 2D ^{1}H HYSCORE spectrum in Figure 3 displays a pair of pronounced ridges (labeled as H-bond I) that are significantly shifted from the antidiagonal. Each ridge extends on both sides of the diagonal such that a small tail of the same ridge is observed in partial overlap with the ridges corresponding to the intrinsic protons (Figure 3). The separation of each ridge such that it extends on either side of the diagonal is due to presence of a "blind spot" at the proton Zeeman frequency. The shift of the ridges from the antidiagonal is attributed to the highly anisotropic (orientation-dependent) dipolar nature of the electron−nuclear hyperfine interaction between A_{1A}^- and the interacting proton. This is characteristic of the presence of a through-space H-bonding interaction. Thus, we assign the ridge H-bond I to the hyperfine interaction of A_{1A}^- with a H-bonded proton from the surrounding protein matrix of PS I.[5] Although the ridges in the spectrum appear to arise from a single H-bond, the possibility that two H-bonds of exactly the same strength between the protein backbone and phylloquinone cannot be ruled out. However, the presence of two H-bonds of equal strength (and geometry) is highly unlikely and is not supported by transient EPR spectroscopy experiments[13,14] and theoretical calculations (see ref 14). Furthermore, the a_{iso} value of the methyl proton obtained here (9.94 ± 0.2 MHz) is larger than that obtained by ENDOR studies of phylloquinone in methanol (7.9 MHz).[9] This indicates the presence of significant spin density at the ring carbon, C_2, associated with the methyl group and points to the presence of an asymmetric H-bonding pattern.

A 2D ^{1}H HYSCORE spectrum of chemically oxidized PS I was recorded (Figure 2S in the Supporting Information) to ensure that the hyperfine interactions to the proton nuclei of the P_{700}^+ state do not contribute to 2D ^{1}H HYSCORE spectrum of photoaccumulated PS I. As can be seen in Figure 2S, the only spectral features that can be detected in chemically oxidized PS I containing the P_{700}^+ radical are due to magnetic interactions with surrounding ^{14}N nuclei. These features are absent in the 2D HYSCORE spectrum of photoaccumulated PS I (Figure 1S in the Supporting Information), suggesting that A_{1A}^- is the only species that is observed in the spectrum depicted in Figure 3 and Figure 1S.

The linear analysis of the 2D ^{1}H HYSCORE spectrum is shown in Figure 4. As expected, the cross-peaks straighten out in the squared-frequency plot (Figure 4a). The points taken from the middle of the ridges attributed to the H-bond can be fit to a straight line (Figure 4b) with slope and intercept of −1.12 and 476.91 MHz^2. Values of a_{iso} and T were calculated as −0.27 ± 0.1 MHz and 3.93 ± 0.07 MHz, respectively (Table1). The numerical simulation using these parameters accurately reproduces the experimental 2D ^{1}H HYSCORE spectrum (Figure 5a) as demonstrated in the corresponding simulated spectrum in Figure 5b. Assuming a spin density of 0.2 on the carbonyl oxygen of the A_{1A}^- semiquinone[14] and using a point-dipole approximation for the electron−nuclear dipolar interaction, the distance between the carbonyl group of the A_{1A}^- and the H-bonded proton is roughly estimated to be 1.6 ± 0.1 Å. This is in excellent agreement with the H-bond length of 1.56 Å estimated based on density function theory (DFT) calculations and optimization of H-bond geometry within the binding pocket.[23] It should be noted that the H-bond length measured here differs from that estimated from the X-ray crystal structure (1.75 Å).[6,24] This might be due to the structural modifications that occur due to the reduction of the quinone to its anionic state.

On the basis of the a_{iso} value obtained from the linear analysis (and confirmed by the numerical simulation) of the 2D ^{1}H

Table 1. Hyperfine Coupling Parameters Obtained from the Analysis of the 2D ^{14}N and ^{1}H HYSCORE Spectra

ridge	T (MHz)	a_{iso} (MHz)	$A_{\perp}$, $A_{\parallel}$ (MHz)	K (MHz)	η
methyl protons	1.33 ± 0.2	9.94 ± 0.2	8.61 ± 0.2, 12.61 ± 0.2		
H-bond I	3.93 ± 0.07	−0.27 ± 0.1	−4.20 ± 0.1, 7.59 ± 0.1		
peptide nitrogen	0.15−0.19	0.75−1.2		0.64−0.72	0.5−1

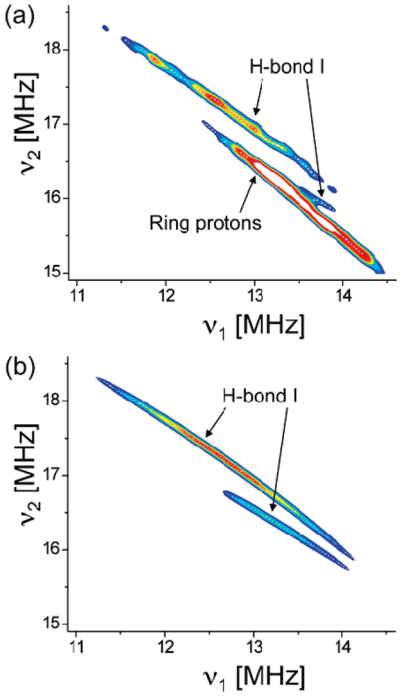

Figure 5. The (+,+) quadrant of the (a) experimental and (b) simulated 2D ^{1}H HYSCORE spectrum of PS I photoaccumulated at pH 8. In order to highlight the ridges arising from the H-bonded proton, the simulation solely depicts this interaction.

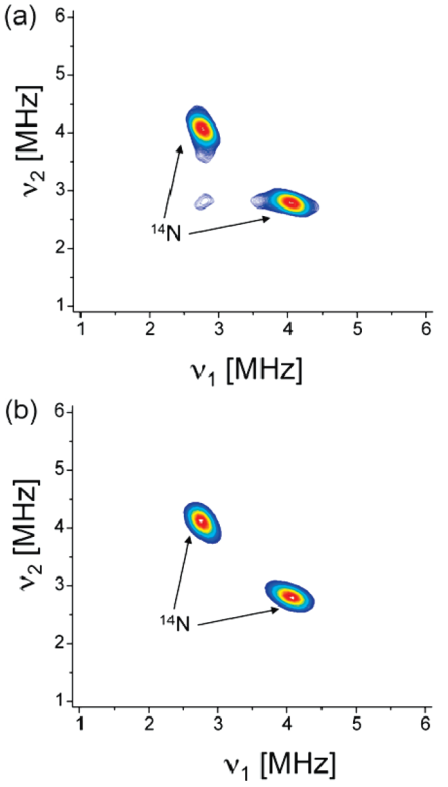

Figure 6. The (+,+) quadrant of the (a) experimental and (b) simulated 2D ^{14}N HYSCORE spectrum of PS I photoaccumulated at pH 8.

HYSCORE spectrum, inferences can be drawn about the geometry of H-bonds to A_{1A}. The hyperfine interactions of semiquinone anions in protic and aprotic solvents have previously been characterized by ENDOR and 2D HYSCORE spectroscopy.[25−27] In a protic solvent, the H-bond formed *in vitro* between the carbonyl oxygen atom of an unsubstituted semiquinone, and the solvent is in-plane with the π-orbitals of the carbonyl keto oxygen atom. In this case, the hyperfine interaction is purely anisotropic in nature with negligible isotropic hyperfine coupling constants. In the case of a semiquinone with substituents on the carbon atom adjacent to the carbonyl groups, as is the case for the A_{1A} phylloquinone, there exists the possibility that an out-of-plane H-bond could be formed.[20] With the increasing nonplanarity, spin density is partially transferred from p-orbital of the carbonyl keto oxygen of the semiquinone radical to the p-orbital of the H-bonding partner.[28] The exchange interaction between the H-bonded partners leads to negative spin density at the corresponding H-bonded hydrogen nucleus, resulting in negative isotropic hyperfine coupling. Thus, on the basis of the negative a_{iso} value of H-bond observed in this study, we conclude that H-bond I is nonplanar.[28] This is consistent with the X-ray crystal structure that depicts the H-bond is at an angle of ∼33° with respect to the quinone plane.[24] A similar nonplanarity is also suggested by DFT calculations.[23]

In this study, 2D ^{14}N HYSCORE spectroscopy was performed to assign the putative H-bond donor of the semiquinone anion state of PS I at pH 8.0. Figure 6a depicts the (+, +) quadrant of the 2D ^{14}N HYSCORE spectrum of PS I photoaccumulated at pH 8.0. A pair of symmetric ridges are observed in the 2D ^{14}N HYSCORE spectrum in Figure 6a with signal intensity at (2.76, 4.06) MHz and (4.06, 2.76) MHz, respectively, and correspond to the double quantum transitions of a ^{14}N nucleus that is in magnetic interaction with the A_{1A}^{-} semiquinone. (These ridges are observed as two intense peaks in the skyline plot (Figure 3S, Supporting Information).) Theoretically, the ridges from the double quantum transitions of a noninteracting nucleus are located on the diagonal at twice the ^{14}N Zeeman frequency ($2\nu_I$ = 2.127 MHz). In the 2D ^{14}N HYSCORE spectrum in Figure 6a, the observed spectral shifts along the diagonal and the antidiagonal are due to the nuclear quadrupole and electron−nuclear hyperfine interactions, respectively. The values of a_{iso}, T, the nuclear quadrupole coupling constant, K, and the asymmetry parameter of the electric field gradient, η, were obtained from comparison of the experimental and simulated (Figure 6b) spectra (Table 1).

The ^{14}N quadrupolar coupling parameters obtained in this study are in agreement with those reported for a peptide nitrogen

of polyglycine, $K = 0.77$ and $\eta = 0.76$.[29] This suggests that the ridges observed in the 2D ^{14}N HYSCORE spectrum in Figure 6a could arise from the peptide nitrogen. The large value of a_{iso} indicates the presence of significant electron spin density on the nitrogen atom. This requires partial overlap with the electron wave function of the phyllosemiquinone and strongly suggests the presence of a H-bonding interaction between the semiquinone anion and the nitrogen atom. This confirms the assignment of the anisotropic dipolar interaction from the H-bonded proton in the 2D ^{1}H HYSCORE spectrum.

It is important to note that the X-ray crystal structure of PS I[6] shows the presence of two nitrogen atoms in the vicinity of A_{1A} that could interact with the semiquinone anion: the indole nitrogen atom of $W697_{PsaA}$ and the peptide amide nitrogen atom of $L722_{PsaA}$. The K and η values obtained from the spectral simulations in the present study do not support the assignment of the ridges in the 2D ^{14}N HYSCORE spectrum as arising from the indole nitrogen atom of a Trp residue, $K = 0.75$ and $\eta = 0.18$.[30] Although the presence of a π-stacking interaction with the phyllosemiquinone could affect the quadrupole coupling parameters, such a strong change of the asymmetry parameter η (as observed here) would require a significant perturbation of the electronic structure of the Trp residue. This precludes the assignment of the ridges in Figure 6 to electron−nuclear hyperfine interaction of A_{1A}^- with the indole nitrogen atom of the Trp residue. Thus, we assign the ^{14}N coupling observed here to the backbone nitrogen of L722 of the PsaA subunit of PS I.

Previous studies[31] using 1D electron spin-echo envelope modulation (ESEEM) spectroscopy study suggested magnetic interactions of the phyllosemiquinone radical with two nitrogen nuclei in the surrounding protein matrix: a strongly coupled indole nitrogen of a Trp residue and a weakly coupled amino nitrogen of a His residue. The difference in the assignments could be due to the limited resolution that is afforded by 1D ESEEM spectroscopy. The application of 2D HYSCORE spectroscopy provides enhanced resolution that allows for unambiguous assignment of the interacting ^{14}N nuclei.

The unambiguous determination of the number and strength of the H-bonds between the protein matrix and the phyllosemiquinone has profound implications on understanding the functional traits of this cofactor in PS I. It has been suggested that a H-bond could contribute as little as +50 mV[4] to as much as +250 mV[32] to the midpoint potential of the phyllosemiquinone/phylloquinone pair. This is counterproductive in a binding pocket that is primarily designed to maintain the quinone at a reducing midpoint potential. Recently, an alternative role for the H-bond has been suggested.[7] The H-bond is proposed to tie up the carbonyl group of the quinone and prevent double reduction/protonation of the quinone that would render it incapable of participating in electron transfer. The quinones in the Q_A site of the purple bacterial reaction center (pbrc) and in photosystem II are comparatively more oxidizing than the quinone in PS I and form two H-bonds. Apart from a H-bond of similar planarity and length formed between the quinone and the protein backbone in the Q_A site of the pbrc, the quinone also forms a second, strong H-bond with an amino side chain (His M219).[13] The presence of a second, strong H-bond (along with other contributing factors such as polarity of the binding pocket, electrostatic interaction, etc.) serves to maintain the quinone in the Q_A site at a significantly more oxidizing potential than in PS I. Therefore, it is clear that the H-bond plays a key role in the quinone binding pocket.

CONCLUSIONS

In this study we have demonstrated that A_{1A}^- phyllosemiquinone in photoaccumulated PS I forms a single, nonplanar H-bond, and we have shown that HYSCORE spectroscopy can be used to probe its semiquinone anionic state. This technique offers the ability to delineate the properties of the H-bond as well as identify any structural differences that may arise as a result of reduction of the quinone without the spectral congestion that is often associated with similar spectroscopic techniques.

ASSOCIATED CONTENT

Supporting Information. 2D HYSCORE spectra displaying the (+,+) and (−,+) quadrants of the A_{1A}^- and chemically oxidized P_{700}^+ state and a skyline plot of the cross-peaks obtained in the 2D HYSCORE spectrum of PS I photoaccumulated at pH 8.0. This material is available free of charge via the Internet at http://pubs.acs.org.

AUTHOR INFORMATION

Corresponding Author

*Phone: (518) 276 3271. Fax: (518) 276 4887. E-mail: lakshk@rpi.edu.

Funding Sources

This work was supported by a grant from the National Science Foundation (MCB-1021725) (J.H.G.) and the United States Department of Energy ((DE-FG-02-98-ER20314) (J.H.G.) and (DE-FG02-0ER06-15) (K.V.L.)).

ABBREVIATIONS

A_1,phylloquinone electron acceptor of photosystem I; PS I, photosystem I; HYSCORE,hyperfine sublevel correlation; ENDOR,electron nuclear double resonance spectroscopy; EPR,electron paramagnetic resonance spectroscopy; H-bond,hydrogen bond.

REFERENCES

(1) Joliot, P., and Joliot, A. (1999) *In vivo* analysis of the electron transfer within Photosystem I: are the two phylloquinones involved?. *Biochemistry 38*, 11130–11136.

(2) Agalarov, R., and Brettel, K. (2003) Temperature dependence of biphasic forward electron transfer from the phylloquinone(s) A_1 in Photosystem I: only the slower phase is activated. *Biochim. Biophys. Acta 1604*, 7–12.

(3) Schlodder, E., Falkenberg, K., Gergeleit, M., and Brettel, K. (1998) Temperature dependence of forward and reverse electron transfer from A_1^-, the reduced secondary electron acceptor in Photosystem I. *Biochemistry 37*, 9466–9476.

(4) Ishikita, H., and Knapp, E. W. (2003) Redox potential of quinones in both electron transfer branches of Photosystem I. *J. Biol. Chem. 278*, 52002–52011.

(5) Ptushenko, V. V., Cherepanov, D. A., Krishtalik, L. I., and Semenov, A. Y. (2008) Semi-continuum electrostatic calculations of redox potentials in Photosystem I. *Photosynth. Res. 97*, 55–74.

(6) Jordan, P., Fromme, P., Witt, H. T., Klukas, O., Saenger, W., and Krauss, N. (2001) Three dimensional structure of Photosystem I at 2.5 Å resolution. *Nature 411*, 909–917.

(7) Srinivasan, N., Karyagina, I., Bittl, R., van der Est, A., and Golbeck, J. H. (2009) Role of the hydrogen bond from Leu722 to the A_{1A} phylloquinone in Photosystem I. *Biochemistry 48*, 3315–3324.

(8) Muhiuddin, I. P., Heathcote, P., Carter, S., Purton, S., Rigby, S. E., and Evans, M. C. (2001) Evidence from time-resolved studies of the $P_{700}^{\cdot+}A_1^{\cdot-}$ radical pair for photosynthetic electron transfer on both

the PsaA and PsaB branches of the Photosystem I reaction centre. *FEBS Lett. 503*, 56–60.

(9) Rigby, S. E., Evans, M. C., and Heathcote, P. (1996) ENDOR and special triple resonance spectroscopy of $A_1^{\cdot-}$ of Photosystem 1. *Biochemistry 35*, 6651–6656.

(10) Purton, S., Stevens, D. R., Muhiuddin, I. P., Evans, M. C., Carter, S., Rigby, S. E., and Heathcote, P. (2001) Site-directed mutagenesis of PsaA residue W693 affects phylloquinone binding and function in the Photosystem I reaction center of *Chlamydomonas reinhardtii*. *Biochemistry 40*, 2167–2175.

(11) Rigby, S. E., Muhiuddin, I. P., Evans, M. C., Purton, S., and Heathcote, P. (2002) Photoaccumulation of the PsaB phyllosemiquinone in Photosystem I of *Chlamydomonas reinhardtii*. *Biochim. Biophys. Acta 1556*, 13–20.

(12) van der Est, A. (2006) Electron transfer involving phylloquinone in Photosystem I, in *Phototosystem I: The Light-Induced Plastocyanin:Ferredoxin Oxidoreductase* (Golbeck, J., Ed.), pp 387−411, Springer, Dordrecht.

(13) Pushkar, Y. N., Golbeck, J. H., Stehlik, D., and Zimmermann, H. (2004) Asymmetric hydrogen-bonding of the quinone cofactor in Photosystem I probed by ^{13}C labeled naphthoquinones. *J. Phys. Chem. B 108*, 9439–9448.

(14) Karyagina, I., Golbeck, J. H., Srinivasan, N., Stehlik, D., and Zimmermann, H. (2006) Single-sided hydrogen bonding to the quinone cofactor in Photosystem I probed by selective ^{13}C labeled naphthoquinones and transient EPR. *Appl. Magn. Reson. 30*, 287–310.

(15) Pushkar, Y. N., Stehlik, D., van Gastel, M., and Lubitz, W. (2004) An EPR/ENDOR study of the asymmetric hydrogen bond between the quinone electron acceptor and the protein backbone in Photosystem I. *J. Mol. Struct. 700*, 233–241.

(16) Niklas, J., Epel, B., Antonkine, M. L., Sinnecker, S., Pandelia, M. E., and Lubitz, W. (2009) Electronic structure of the quinone radical anion A_1^- of Photosystem I investigated by advanced pulse EPR and ENDOR techniques. *J. Phys. Chem. B 113*, 10367–10379.

(17) Johnson, T. W., Shen, G., Zybailov, B., Kolling, D., Reategui, R., Beauparlant, S., Vassiliev, I. R., Bryant, D. A., Jones, A. D., Golbeck, J. H., and Chitnis, P. R. (2000) Recruitment of a foreign quinone into the A_1 site of Photosystem I. I. Genetic and physiological characterization of phylloquinone biosynthetic pathway mutants in *Synechocystis* sp. PCC 6803. *J. Biol. Chem. 275*, 8523–8530.

(18) Lakshmi, K. V., Jung, Y. S., Golbeck, J. H., and Brudvig, G. W. (1999) Location of the iron-sulfur clusters F_A and F_B in Photosystem I: an electron paramagnetic resonance study of spin relaxation enhancement of P_{700}^+. *Biochemistry 38*, 13210–13215.

(19) Weyers, A. M., Chatterjee, R., Milikisiyants, S., and Lakshmi, K. V. (2009) Structure and function of quinones in biological solar energy transduction: A differential pulse voltammetry, EPR, and hyperfine sub-level correlation (HYSCORE) spectroscopy study of model benzoquinones. *J. Phys. Chem. B 113*, 15409–15418.

(20) Dikanov, S. A., Samoilova, R. I., Kolling, D. R., Holland, J. T., and Crofts, A. R. (2004) Hydrogen bonds involved in binding the Q_i-site semiquinone in the bc1 complex, identified through deuterium exchange using pulsed EPR. *J. Biol. Chem. 279*, 15814–15823.

(21) Rohrer, M., MacMillan, F., Prisner, T. F., Gardiner, A. T., Möbius, K., and Lubitz, W. (1998) Pulsed ENDOR at 95 GHz on the primary acceptor ubisemiquinone in photosynthetic bacterial reaction centers and related model systems. *J. Phys. Chem. B 102*, 4648–4657.

(22) Stoll, S., and Schweiger, A. (2006) EasySpin, a comprehensive software package for spectral simulation and analysis in EPR. *J. Magn. Reson. 178*, 42–55.

(23) Teutloff, C., Bittl, R., and Lubitz, W. (2004) Pulse ENDOR studies on the radical pair $P_{700}^{+\cdot}$ $A_1^{\cdot-}$ and the photoaccumulated quinone acceptor $A_1^{\cdot-}$ of Photosystem I. *Appl. Magn. Reson. 26*, 5–21.

(24) Fromme, P., Jordan, P., and Krauss, N. (2001) Structure of Photosystem I. *Biochim. Biophys. Acta 1507*, 5–31.

(25) MacMillan, F., Lendzian, F., and Lubitz, W. (1995) EPR and ENDOR characterization of semiquinone anion radicals related to photosynthesis. *Magn. Reson. Chem. 33*, 581–593.

(26) Flores, M., Isaacson, R. A., Calvo, R., Feher, G., and Lubitz, W. (2003) Probing hydrogen bonding to quinone anion radicals by ^1H and ^2H ENDOR spectroscopy at 35 GHz. *Chem. Phys. 294*, 401–413.

(27) O'Malley, J. P., and Babcock, G. T. (1986) Powder ENDOR spectra of p-benzoquinone anion radical: Principal hyperfine tensor components for ring protons and for hydrogen-bonded protons. *J. Am. Chem. Soc. 108*, 3995–4001.

(28) O'Malley, J. P. (1998) A density functional study of the effect of orientation of hydrogen bond donation on the hyperfine couplings of benzosemiquinones: Relevance to semiquinone−protein hydrogen bonding interactions in vivo. *Chem. Phys. Lett. 291*, 367–374.

(29) Blinc, R., Mali, M., Osredkar, R., Seliger, J., and Ehrenberg, L. (1974) ^{14}N quadrupole resonance in polyglycine. *Chem. Phys. Lett. 28*, 158–159.

(30) Edmonds, D. T. (1977) Nuclear quadrupole double resonance. *Phys. Rep. 29*, 233–290.

(31) Hanley, J., Deligiannakis, Y., MacMillan, F., Bottin, H., and Rutherford, A. W. (1997) ESEEM study of the phyllosemiquinone radical A_1^- in ^{14}N and ^{15}N labeled Photosystem I. *Biochemistry 36*, 11543–11549.

(32) O'Malley, P. J. (1999) Density functional calculated spin densities and hyperfine couplings for hydrogen bonded 1,4-naphthosemiquinone and phyllosemiquinone anion radicals: a model for the A_1 free radical formed in Photosystem I. *Biochim. Biophys. Acta 1411*, 101–113.